FTIR Imaging of Polymeric Materials under High-Pressure Carbon Dioxide

Sergei G. Kazarian* and K. L. Andrew Chan

Department of Chemical Engineering and Chemical Technology, Imperial College London, London SW7 2AZ, UK

Received September 22, 2003; Revised Manuscript Received November 3, 2003

ABSTRACT: A novel application of FTIR imaging to study polymers subjected to high-pressure CO_2 was demonstrated. FTIR images of polymer blends under high-pressure CO_2 were obtained in situ using a single reflection ATR diamond accessory combined with a high-pressure cell. Two systems, a polystyrene (PS)/poly(vinyl methyl ether (PVME) blend and a poly(ethylene oxide) (PEO)/poly(methyl methacrylate) (PMMA) system, have been studied to demonstrate the feasibility and principles of this new approach. Using this approach, the CO_2-induced phase separation of an initially homogeneous PS/PVME blend was observed at a CO_2 pressure of 60 bar and temperature of 40 °C. FTIR imaging allowed us to identify formation of distinct domains that are PS- and PVME-rich. The size of these domains was ca. 200 μm. In a second high-pressure imaging experiment, the interfacial region between PEO and PMMA was studied. Sorption of high-pressure CO_2 in both polymers was studied simultaneously. The effect of temperature and pressure on the solubility of CO_2 in PMMA and PEO was demonstrated. The sorption of CO_2 in PEO reduced the melting point of the polymer which facilitated an increase in CO_2 sorption. The successful demonstration of this novel spectroscopic imaging approach under high pressure opens up new possibilities for studying polymeric materials subjected to high-pressure gases and supercritical fluids.

Introduction

Applications of supercritical CO_2 in polymer processing are partly driven by environmental concerns. It was demonstrated, however, that the intrinsic properties of CO_2 can induce beneficial changes in polymers for enhanced processing of polymeric materials.[1] This includes CO_2-induced plasticization,[2,3] swelling,[4−6] foaming, crystallization, viscosity reduction, mixing, and impregnation.[1,7] Therefore, there is a continuing need to study the effects of CO_2 on polymers. In particular, the effects of high-pressure CO_2 on the morphology of polymer blends have recently received much attention[8−12] and were discussed in recent reviews.[1,7] Visualization of polymer morphologies and spatial distribution of different components in polymeric materials are needed in order to optimize processing routes. Therefore, polymer scientists and engineers will benefit from the method of high-pressure FTIR imaging introduced in this paper.

FTIR spectroscopy has proven to be a powerful tool to study polymeric materials subjected to high-pressure or supercritical (sc) CO_2. In situ monitoring using FTIR spectroscopy helps to optimize high-pressure supercritical fluid processes. Conventional FTIR spectroscopy probes interactions between supercritical CO_2 and polymers at a molecular level and provides a fundamental understanding of the origin of many effects of $scCO_2$ on polymeric materials (such as plasticization, swelling, etc.). Unfortunately, conventional FTIR spectroscopy lacks the advantage of the most basic photographic camera: obtaining a whole picture in a single snapshot. Therefore, it is not possible to assess chemical heterogeneity of polymeric materials under pressures. Fortunately, new infrared array detectors have been developed recently that incorporate thousands of small detectors in a grid pattern. The use of these array detectors is the basis of FTIR spectroscopic imaging (including ATR imaging[13]) which can obtain the spatial distribution of molecular components in the heterogeneous sample in a single measurement.[14] The applications of FTIR imaging (including an ATR imaging) to characterize a broad range of polymeric materials were discussed recently.[15−21]

The opportunity exists to apply FTIR imaging under pressure to study polymeric materials subjected to $scCO_2$. This opportunity became possible due to recent developments: (i) modification of a single reflection diamond ATR (attenuated total reflection)−IR accessory (Golden Gate) for in situ study of supercritical fluids;[5,22,23] (ii) demonstration of the possibility of obtaining FTIR images using this diamond ATR−IR accessory.[24,25]

Combining a diamond ATR−IR accessory with a miniature high-pressure cell led to the development of this new in situ high-pressure spectroscopic approach.[23] Significant advantages of the approach are that there are no windows to seal, the chemical and physical properties of diamond are favorable, and a small cell volume makes high-pressure experiments safe. This approach was successfully applied to measure the IR spectra of liquefied gases and three types of novel "green" solvents: supercritical carbon dioxide, ionic liquids, and near-critical water.[26] Furthermore, this in situ ATR−IR method allowed simultaneous quantification of CO_2 sorption and corresponding swelling of polymers.[5] However, all these successful applications utilized conventional IR detectors which are suitable for studying homogeneous materials.

Our other recent work[24] realized the possibility of using the same diamond ATR−IR accessory for imaging applications with a nominal spatial resolution of ca. 15 μm. Therefore, an exciting opportunity emerged for imaging of heterogeneous polymeric materials under high pressures by combining a diamond ATR−IR accessory, a miniature high-pressure cell, and an FTIR

* Corresponding author: e-mail s.kazarian@imperial.ac.uk.

10.1021/ma035420y CCC: $27.50
Published on Web 12/18/2003

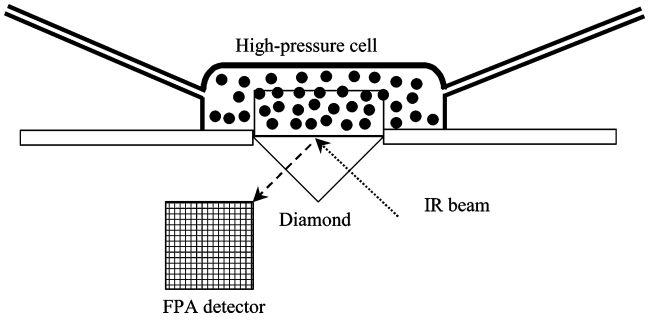

Figure 1. Schematic presentation of a modified diamond ATR−IR accessory for studying polymeric materials subjected to high-pressure carbon dioxide.

imaging system. The feasibility of this method is demonstrated in this paper on two polymeric systems under high-pressure carbon dioxide.

Experimental Section

PS/PVME Blend. A blend of 50/50 wt % of PS (M_w = 100 000) and PVME (M_w = 8000) was prepared by dissolving both polymers in toluene. The solution was cast on the diamond crystal of the diamond ATR−IR accessory "Golden Gate" (Specac Ltd.) and heated to 60 °C for a few hours to remove the residual solvent. The presence of the solvent in the sample was monitored by measuring the FTIR spectra of the sample. The thickness of the film was ca. 8 μm. Once all solvent residues were removed, the sample was cooled to 40 °C for the imaging measurements. The sample was pressurized with CO_2 to 60 bar.

PEO/PMMA System. An interface between PMMA (M_w = 100 000) and PEO (M_w = 6000) was created in two steps. First, a film of PMMA was cast (from solution in CH_2Cl_2) on half of the measuring surface of the diamond crystal with removal of the residual solvent at 60 °C. Then, the PEO was carefully melted on the rest of the diamond surface at 60 °C, forming a contact with but not covering the PMMA film (the quality of contact was monitored via FTIR imaging). The sample was then cooled to 30 °C. The sample was pressurized with CO_2 to 50 bar. The measurements at higher temperatures were made after CO_2 reached equilibrium sorption.

High-Pressure Setup. A high-pressure cell was sealed to the tungsten carbide plate with bridge clamping mechanism of the "Golden Gate" as shown in Figure 1. The CO_2 (99.9% pure, supplied by BOC) pressure was supplied using a high-pressure syringe pump (HiP) and monitored with a pressure gauge.

FTIR Imaging. FTIR images were collected with the system that comprises of an IFS 66/S step-scan FTIR spectrometer (Bruker Optics), a macrochamber extension, and a 64 × 64 focal plane array (FPA) detector. The diamond ATR−IR accessory was positioned in the macrochamber and carefully aligned prior to the measurements.[24] The sample area measured by this macro-ATR imaging approach is ca. 0.8 × 1.1 mm^2. A spectral resolution of 16 cm^{-1} has been used in this study. Twenty frames (frame rate of 180 Hz) were collected in each step to co-add and average for a reasonable signal-to-noise ratio.

Results and Discussion

Images that represent the spatial distribution of different components have been generated by plotting the integral absorbance of the band that characterizes the presence of the component over the whole sampling area.

PS/PVME Blend. This system was chosen because it is a lower critical solution temperature (LCST) blend where the increase in temperature results in phase separation. It was shown that the effect of CO_2 often mimics the effect of the heat.[3] In particular, Watkins and co-workers[27] have demonstrated CO_2-induced phase separation of PS/PVME. In that work, phase separation induced by high-pressure CO_2 was unambiguously confirmed, but it was not possible to visualize the spatial distribution of different phases. Therefore, this blend appeared as a good candidate for a demonstration of the principles of our imaging approach.

It is important to identify characteristic spectral bands for each component that can be used for constructing images of the distribution of specific polymers. The bands at 1077 and 1492 cm^{-1} have been used to characterize PVME and PS, respectively, since these bands do not overlap with other spectral bands and have a reasonable absorbance. The FTIR images showing the distribution of PS in the polymer blend, before and after it was subjected to 60 bar of CO_2, are shown in Figure 2. Before the sample was subjected to CO_2, the distribution of PS and PVME was homogeneous (shown in Figure 2a,c). However, the sample has become inhomogeneous when subjected to 60 bar of CO_2. Under these conditions the sample phase-separated into PS-rich and PVME- rich regions with domain sizes of ca. 200 μm (Figure 2b,d). In regions where the absorbance of the PS band was high, the absorbance of the PVME band was lower as compared with the initial homogeneous sample. Figure 2e shows selected spectra extracted from the PS-rich (red line) and PVME-rich areas (blue line).

Comparing the images generated for the PS before and after pressurizing with CO_2 (Figure 2a,b) shows that the absorbance of the spectral bands is decreased. This reduction in absorbance is also observed in the PS-rich region after the phase separation. The decrease in absorption of PS can be explained by considering the swelling of the polymer under high pressure of CO_2. Swelling of PS under high pressure of CO_2 has been observed by many authors.[4,6,28−31] The density of the polymer decreases as a result of swelling and, hence, the absorbance of the spectral bands also decrease. This effect was demonstrated using conventional ATR−IR spectroscopy.[5] The reduction of absorbance of the spectral bands of PVME was less compared with the bands of PS, apparently due to lower swelling of this polymer. Most importantly, application of FTIR imaging using the ATR−IR approach allowed us to visualize the CO_2-induced phase separation and formation of PS-rich and PVME-rich domains in an initially homogeneous polymer mixture. This result shows that this approach provides a powerful tool to monitor both polymer phase separation in the case of LCST blends and, potentially, the effect of CO_2 on polymer mixing in other systems.

PEO/PMMA System. A system of a semicrystalline and glassy polymer was chosen to demonstrate the possibility of using the in situ ATR−IR imaging approach to study simultaneously sorption of CO_2 in different polymers. Sorption of CO_2 in polymers has been studied extensively because this information is needed in order to understand supercritical CO_2 polymer processing. In situ FTIR spectroscopy of gas sorption has a number of advantages over conventional gravimetric techniques because of chemical specificity of the spectroscopic method.[22,23,26] This in situ imaging approach, however, is the first attempt to measure sorption of CO_2 in different polymers simultaneously due to the ability of imaging with an array detector. The absorbance of the ν(C═O) band of PMMA at 1726 cm^{-1} was used to characterize the distribution of PMMA while the distribution of PEO was represented by the

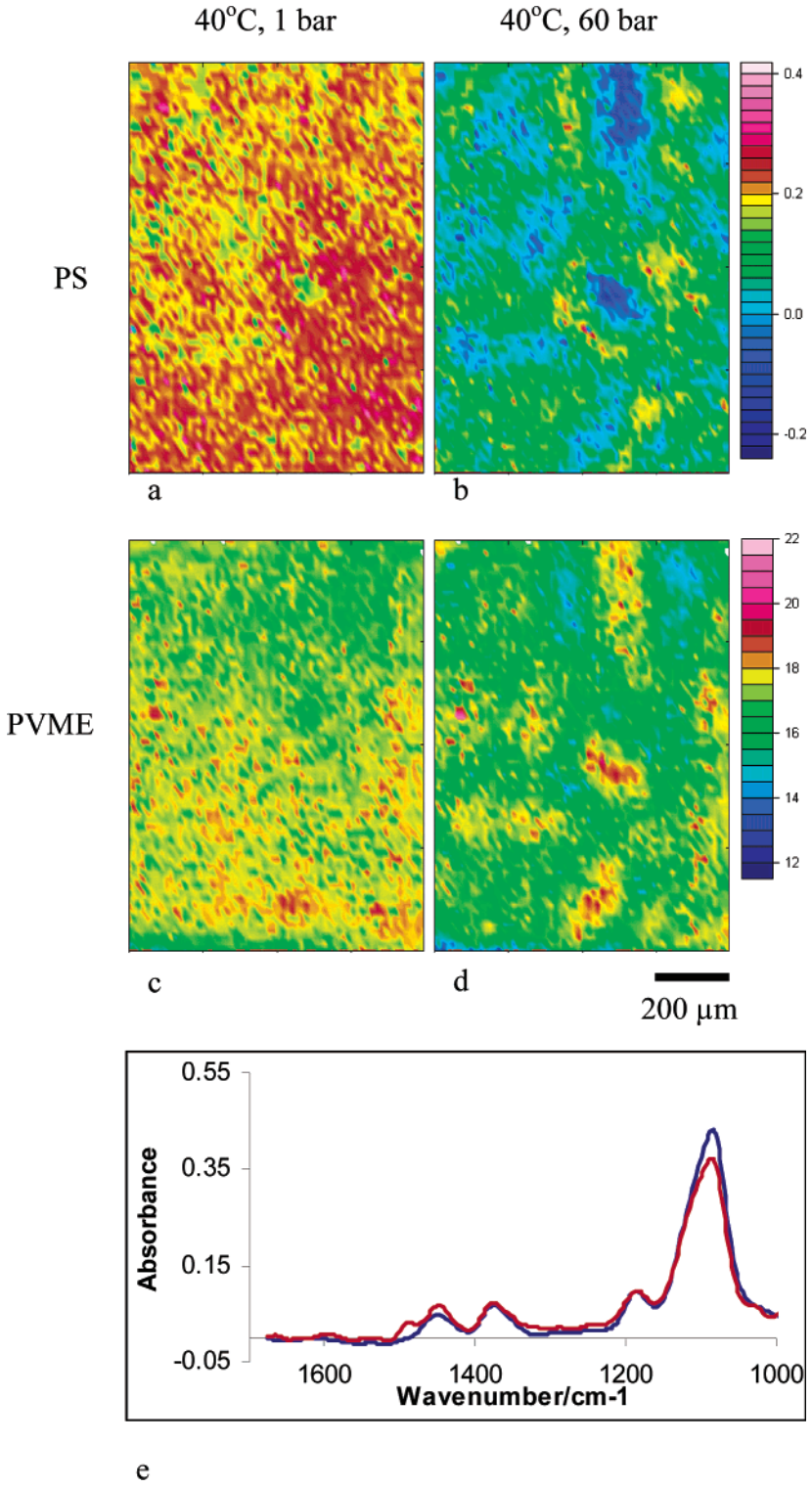

Figure 2. ATR−IR images of PS and PVME blend before (a and c) and during exposure to 60 bar of CO_2 (b and d). Images a and b are based on the spectral band of PS while images c and d are based on the spectral band of PVME. The size of each image is 820 × 1140 μm^2. Part e shows spectra extracted from PVME-rich (blue) and PS-rich (red) domains.

absorbance of the band at 1350 cm^{-1}. The distribution of CO_2 dissolved in the polymers was represented by the absorbance of the ν_3 band of the antisymmetric stretching mode of CO_2 at ca. 2338 cm^{-1}. Figure 3 shows images representing the distribution of PMMA (top row), PEO (middle row), and dissolved CO_2 (bottom row). Each column of images represents the distribution of PMMA, PEO, and CO_2 at the different conditions. The left column of the images shows that the sample preparation resulted in the formation of two distinct domains of pure polymers with a rather sharp interface. Figure 3i shows the absence of CO_2 prior to pressurizing the system. The selected ATR−IR spectra from specific locations shown in Figure 4 were extracted as indicated by the arrows on the images a, b, k, and l in Figure 3. The band position and the band shape (narrow and rather symmetrical band) of CO_2 indicated that this band corresponds to the CO_2 dissolved in the polymer and there was no gaseous CO_2 present (which is evidenced by the lack of rotational branches), confirming

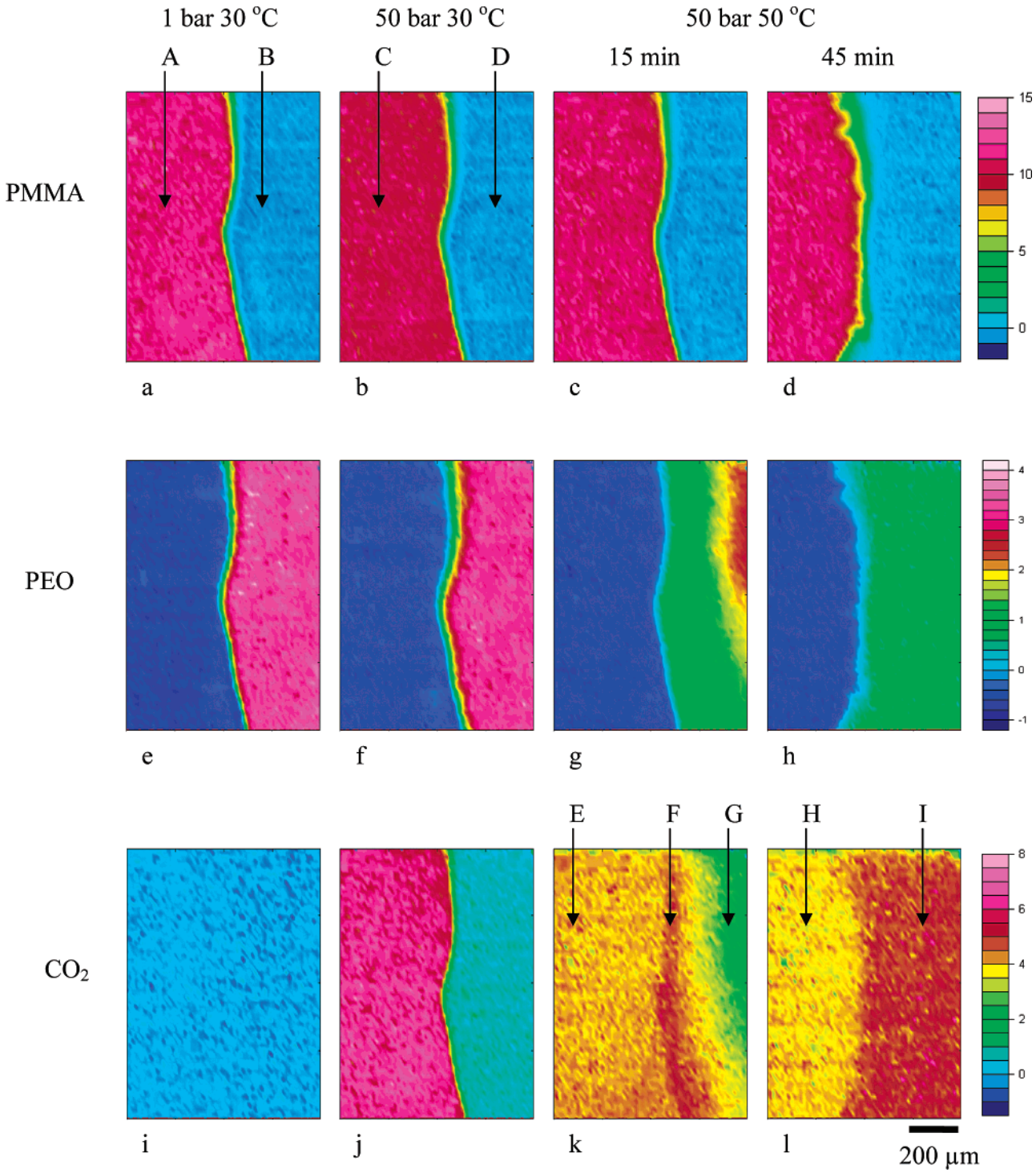

Figure 3. ATR−IR images of the PMMA/PEO system. Top row shows images based on the spectral band of PMMA, middle row shows images based on the spectral band of PEO, and the bottom row shows images based on the spectral band of CO_2 dissolved in polymers. The conditions of the sample are indicated on the top of the images. The ATR−IR spectra extracted at the selected locations (indicated by the capital letters) are shown in Figure 4.

the absence of CO_2 in the interfacial area between the diamond and polymer film which may happen in the case of delaminating of the polymer film. The images of PMMA (Figure 3a−d) demonstrate that the distribution of PMMA does not change as a function of CO_2 pressure or temperature. However, a decrease of the absorbance of the ν(C═O) band of PMMA was observed when the sample was subjected to 50 bar of CO_2 at 30 °C. This was the result of swelling of PMMA under high-pressure CO_2 as observed in spectroscopic experiments with conventional spectroscopy. Furthermore, the absorbance of the spectral bands of PMMA increased when the sample was heated from 30 to 50 °C as can be seen by the change in the absorbance of the ν(C═O) band represented by the color intensity scale in Figure 3b,c. The increase in absorbance of the spectral bands of PMMA was a consequence of a decrease in polymer swelling after heating to 50 °C. This occurred because the solubility of CO_2 in PMMA decreases with increasing temperature. This is consistent with the images of the distribution of CO_2 in PMMA (Figure 3j,k) where the absorbance of the ν_3 band of CO_2, which is propor-

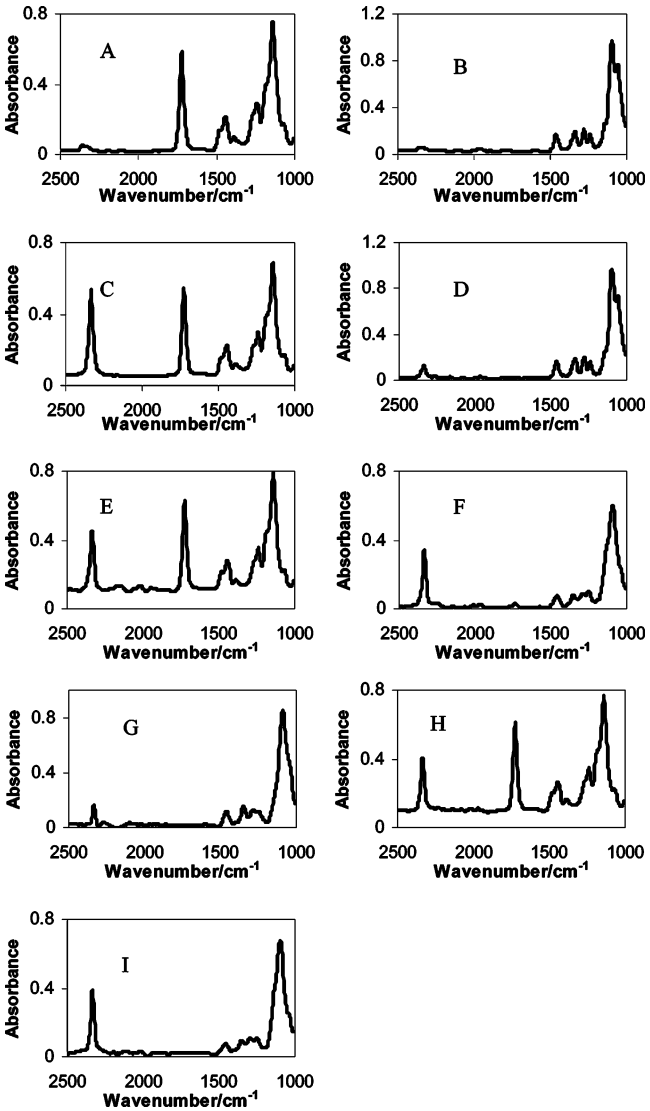

Figure 4. ATR−IR spectra extracted from different area of the sample at different time indicated by the corresponding arrows shown in Figure 3.

tional to the concentration of CO_2, decreased significantly with an increase of temperature from 30 to 50 °C.

The images of PEO indicate that at 30 °C no major change in the distribution of PEO was observed when the sample was pressurized with 50 bar of CO_2. Indeed, analysis of the spectrum extracted from area D demonstrates that the shape of the PEO band at 1095 cm^{-1} corresponds to the solid PEO. Furthermore, the absorbance of the band of CO_2 in PEO was very weak compared to the absorbance of this band of CO_2 dissolved in PMMA under the same conditions (Figure 3j). This indicates a very small sorption of CO_2 in semicrystalline PEO. However, when the temperature is increased to 50 °C, the PEO begins to melt slowly. Apparently, the presence of a small amount of dissolved CO_2 reduces the melting temperature of PEO—the effect is similar to the reduction of melting temperature for poly(ethylene glycol).[26] Figure 3g has shown that the absorbance of PEO decreased after the temperature increased to 50 °C for 15 min. Interestingly, this decrease in absorbance is more pronounced closer to the interface with PMMA, and this is consistent with Figure 3k, which has shown a greater sorption of CO_2 in the regions of PEO which are closer to the interface with PMMA. This can be explained by the presence of diffusion of CO_2 not only from the top of the film but also from the side where the concentration of CO_2 was high. The image obtained after 45 min from the onset of heating the film to 50 °C shows that the distribution of CO_2 has reached equilibrium. The dramatic change in the shape of the band of PEO at 1095 cm^{-1} in the spectrum extracted from the area F with disappearance of the sharp features indicates that PEO has melted. The absorbance of CO_2 has increased significantly in the melt areas of PEO. In fact, more CO_2 is dissolved in the molten PEO than in the PMMA under identical conditions. This comparison also demonstrates the power of this imaging approach because sorption of CO_2 is measured simultaneously in two different polymers under identical conditions. This also points to the possibility of using this approach for high-throughput analysis by studying sorption of CO_2 in many polymers simultaneously. This not only would save time due to fast screening of many samples but also will ensure an enhanced accuracy since all samples will be measured under the same conditions.

Figure 3h shows that the front of PEO moved toward the PMMA region. This could be due to polymer interdiffusion. However, this also could be because the molten PEO flows underneath the PMMA film near the interface. A different sample preparation may help to clarify this issue. Nevertheless, this example also demonstrates the value of this high-pressure imaging method. First, imaging allowed us to elucidate the phenomenon more accurately to avoid misinterpretation of the data which may be possible in this case using conventional spectroscopy. Second, this example also shows that other phenomena, for example CO_2-enhanced polymer interdiffusion, may be studied using the unique possibility offered by this approach.

Conclusions

A novel high-pressure method has been developed which allows chemical imaging of polymeric materials subjected to supercritical CO_2. This method is based on FTIR imaging combined with a diamond ATR−IR accessory[24] that allows in situ measurements of high-pressure gases and supercritical fluids. Spatial information on the polymer sample with a resolution of ca. 15 μm can be obtained in situ under high pressures. The demonstrated ability of this imaging approach to study simultaneously different polymers subjected to high-pressure CO_2 opens up new research opportunities in supercritical fluid research.

This study showed that the imaging approach allowed us to visualize the phase separation of a PS/PVME blend induced by high-pressure CO_2. The formation of PS-rich and PVME-rich domains was detected under 60 bar of CO_2 in an initially homogeneous polymer blend. In a second example, PMMA and PEO were studied at different temperatures and pressures of CO_2. The differences in CO_2 sorption were monitored along with the detection of the changes in polymers (swelling of PMMA and melting of PEO).

The approach demonstrated in this paper is applicable to the study of multicomponent polymer systems, including blends and composite materials, subjected to high-pressure CO_2. The ability to visualize in a novel manner the effects of CO_2-induced plasticization, swelling, melting, crystallization, mixing, or phase separation

opens up new research opportunities. The approach presented here also shows promise for in situ visualization of particle-filled polymeric materials where the exposure to high-pressure CO_2 affects their rheological behavior and processing conditions.[32] This imaging approach is not limited to materials subjected to CO_2, since it is possible to study the effects of other gases on different polymers simultaneously although in order to directly monitor gas sorption, the gas molecules need to be IR-active. The success of this study opens up the possibility to apply this imaging approach to investigate the effect of near-critical and supercritical water on complex polymeric materials. A tremendous potential exists to apply this in situ spectroscopic imaging approach to high-throughput analysis under high temperatures and pressures, and this study is the first step toward realization of this potential.

Acknowledgment. We are grateful to EPSRC, Bruker Optics, and Specac Ltd. for support. We thank Drs. P. Turner and G. Poulter for their help and advice.

References and Notes

(1) Kazarian, S. G. *J. Polym. Sci., Ser. C* **2000**, *42*, 78−101.
(2) Condo, P. D.; Johnston, K. P. *J. Polym. Sci., Part B: Polym. Phys.* **1994**, *32*, 523−533.
(3) Kazarian, S. G.; Brantley, N. H.; West, B. L.; Vincent, M. F.; Eckert, C. A. *Appl. Spectrosc.* **1997**, *51*, 491−494.
(4) Wissinger, R. G.; Paulaitis, M. E. *Ind. Eng. Chem. Res.* **1991**, *30*, 842−851.
(5) Flichy, N. M. B.; Kazarian, S. G.; Lawrence, C. J.; Briscoe, B. J. *J. Phys. Chem. B* **2002**, *106*, 754−759.
(6) Tadanori, K.; Seo, Y.-S.; Shin, K.; Zhang, Y.; Rafailovich, M. H.; Sokolov, J. C.; Chu, B.; Satija, S. K. *Macromolecules* **2003**, *36*, 5236−5243.
(7) Tomasko, D. L.; Li, H.; Liu, D.; Han, X.; Wingert, M. J.; Lee, L. J.; Koelling, K. W. *Ind. Eng. Chem. Res.* **2003**, *42*, 6431−6456.
(8) Watkins, J. J.; Brown, G. D.; Ramachandrarao, V. S.; Pollard, M. A.; Russell, T. P. *Macromolecules* **1999**, *32*, 7737−7740.
(9) Siripurapu, S.; Gay, Y. J.; Royer, J. R.; DeSimone, J. M.; Spontak, R. J.; Khan, S. A. *Polymer* **2002**, *43*, 5511−5520.
(10) Lee, M.; Tzoganakis, C.; Park, C. B. *Adv. Polym. Technol.* **2000**, *19*, 300−311.
(11) Elkovich, M. D.; Lee, L. J.; Tomasko, D. L. *Polym. Eng. Sci.* **2001**, *41*, 2108−2125.
(12) Walker, T. A.; Melnichenko, Y. B.; Wignall, G. D.; Spontak, R. J. *Macromolecules* **2003**, *36*, 4245−4249.
(13) Burka, E. M.; Curbelo, R. US Patent 6,141,100, 2000.
(14) Kidder, L. H.; Haka, A. S.; Lewis, E. N. In *Handbook of Vibrational Spectroscopy*; Chalmers, J. M., Griffiths, P. R., Eds.; John Wiley & Sons: Chichester, 2002; Vol. 2, pp 1386−1404.
(15) Koenig, J. *Adv. Mater.* **2002**, *14*, 457−460.
(16) Miller-Chou, B. A.; Koenig, J. L. *Macromolecules* **2003**, *36*, 4851−4861.
(17) Gupper, A.; Wilhelm, P.; Schmied, M.; Kazarian, S. G.; Chan, K. L. A.; Reussner, J. *Appl. Spectrosc.* **2002**, *56*, 1515−1523.
(18) Artyushkova, K.; Wall, B.; Koenig, J. L.; Fulghum, J. E. *J. Vac. Sci. Technol. A* **2001**, *19*, 2791−2799.
(19) Kazarian, S. G.; Higgins, J. S. *Chem. Ind.* **2002**, *10*, 21−23.
(20) Snively, C. M.; Koenig, J. L. *Macromolecules* **1998**, *31*, 3753−3755.
(21) Kazarian, S. G.; Chan, K. L. A. *Macromolecules* **2003**, *36*, 9866−9872.
(22) Kazarian, S. G.; Briscoe, B. J.; Coombs, D.; Poulter, G. *Spectrosc. Eur.* **1999**, *11*, 10−16.
(23) Kazarian, S. G.; Flichy, N. M. B.; Coombs, D.; Poulter, G. *Am. Lab.* **2001**, *33*, 44−49.
(24) Chan, K. L. A.; Kazarian, S. G. *Appl. Spectrosc.* **2003**, *57*, 381−389.
(25) Chan, K. L. A.; Hammond, S. V.; Kazarian, S. G. *Anal. Chem.* **2003**, *75*, 2140−2147.
(26) Kazarian, S. G. *Macromol. Symp.* **2002**, *184*, 215−228.
(27) Ramachandrarao, V. S.; Watkins, J. J. *Macromolecules* **2000**, *33*, 5143−5152.
(28) Chang, S. H.; Park, S. C.; Shim, J. J. *J. Supercrit. Fluids* **1998**, *13*, 113−119.
(29) Wissinger, R. G.; Paulaitis, M. E. *J. Polym. Sci., Part B: Polym. Phys.* **1987**, *25*, 2497−2510.
(30) Hilic, S.; Boyer, S. A. E.; Padua, A. A. H.; Grolier, J. P. E. *J. Polym. Sci., Part B: Polym. Phys.* **2001**, *39*, 2063−2070.
(31) Nikitin, L. N.; Gallyamov, M. O.; Vinokur, R. A.; Nikolaev, A. Y.; Said-Galiyev, E. E.; Khokhlov, A. R.; Jespersen, H. T.; Schaumburg, K. *J. Supercrit. Fluids* **2003**, *26*, 263−273.
(32) Flichy, N. M. B.; Lawrence, C. J.; Kazarian, S. G. *Ind. Eng. Chem. Res.* **2003**, *42*, 6310−6319.

MA035420Y